

## TWO HIGH-BETA TOROIDAL CONFIGURATIONS: A STELLARATOR AND A TOKAMAK-TORSATRON HYBRID

A.H. BOOZER, T.K. CHU, R.L. DEWAR\*, H.P. FURTH,  
J.A. GOREE, J.L. JOHNSON†, R.M. KULSRUD,  
D.A. MONTICELLO, G. KUO-PETRAVIC,  
G.V. SHEFFIELD, S. YOSHIKAWA  
Plasma Physics Laboratory,  
Princeton University,  
Princeton, New Jersey

O. BETANCOURT  
Courant Institute of Mathematics,  
New York University,  
New York, N.Y.

United States of America

### Abstract

#### TWO HIGH-BETA TOROIDAL CONFIGURATIONS: A STELLARATOR AND A TOKAMAK-TORSATRON HYBRID.

Two novel modular-coil toroidal confinement systems are presented, both having simple coil structures, quasi-helical symmetry, and a potential for stable high-beta confinement. The tokatron is a highly elongated tokamak with finite vacuum-field rotational transform provided by twisting the toroidal field coils so as to lie in surfaces with vertically oriented screw symmetry. The heliac consists of an  $\ell = 1$  helical field superimposed on the poloidal field produced by a current-carrying toroidal conductor. It has a magnetic well even in the limit of large-aspect-ratio  $R/a$ .

#### 1. TOKATRON

The addition of a torsatron vacuum field to the tokamak configuration can serve to enhance stability against ballooning and resistive kink modes. In order for the tokamak poloidal field to contribute significantly, in turn, to stability and plasma confinement, a toroidal configuration with low aspect ratio  $R/a$  and with large vertical elongation  $b/a$  is desirable. These conditions tend to conflict with conventional stellarator/torsatron symmetry, i.e.  $\vec{B} = \vec{B}(r, \theta - kR\phi)$ , where  $r$  is the minor

\* Present address: Australian National University, Canberra, Australia.

† On loan from Westinghouse Research and Development Center,  
Pittsburgh, PA 15235, USA.

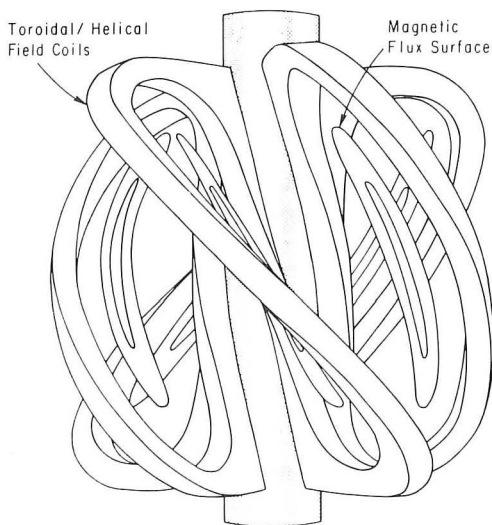


FIG.1. Tokamak configuration.

radius and  $\theta$  and  $\phi$  are the poloidal and toroidal angles. This contradiction can be resolved by twisting the toroidal field coils to form a torsatron winding (Fig. 1) with screw symmetry pointing along the  $z$ -axis, rather than along the toroidal minor axis, i.e.:  $\vec{B} = \vec{B}(R, \phi - kz)$ . In that case,  $R/a$  can be arbitrarily low; perfect symmetry is achieved in the limit  $b/a \rightarrow \infty$ . The coils lie in screw planes  $\phi = \phi_0 + kz$ ; they are modular and topologically unentangled.

To produce a closed tokatron vacuum-field configuration, an external vertical field is superimposed, as in the related case of "semi-stellarator" fields described in Ref. [1]. The presence of the vacuum field facilitates the maintenance of highly elongated tokamak plasmas in positionally stable equilibrium, as in the plasma configurations of Ref. [2]. The presence of the plasma current, in turn, serves to alleviate symmetry-spoiling finite-length effects on flux surfaces and particle orbits.

Accurate self-consistent equilibria for tokatron configurations can be modeled with asymptotic expansions based on a small helical field. It has been shown that a narrow parameter range exists, such that the helical-field transform can help to shape the minor cross section of the current-carrying plasma, while good magnetic surfaces are maintained [3]. Further particulars concerning the tokatron are given in Ref. [4].

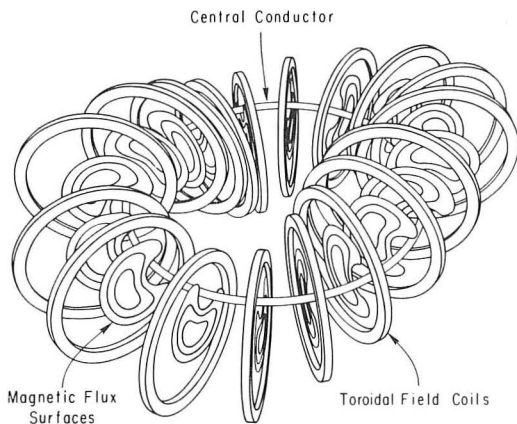


FIG.2. Heliac configuration.

## 2. THE HELIAC

The superposition of an  $\lambda = 1$  torsatron vacuum field on the tokamak-like poloidal field of a current-carrying toroidal conductor produces nested helical flux tubes [5-7] analogous to the magnetic islands that can develop near a rational surface in a tokamak. The minor cross sections of the outer flux surfaces become increasingly kidney-shaped near the edge, with the concave side of the kidney facing the toroidal conductor. Such a configuration can have a deep magnetic well derived from the gradient of the poloidal field [5]. The necessary  $\lambda = 1$  field can be produced by a set of ordinary tokamak TF coils lying in vertical planes with their centers located on a helical curve around the central conductor (Fig. 2). The current-carrying toroidal conductor markedly increases the rotational transform, allowing shorter connection length between regions of favorable and unfavorable curvature, and provides large local shear, thus improving the beta. The centers of the TF coils are on a helical path  $\phi = -N\theta$ , with  $\phi$  and  $\theta$  the toroidal and poloidal angles and  $N$  the number of periods. The heliac differs from earlier stellarators with nonplanar axes [8-12] in having a current in the central conductor to create a vacuum-field magnetic well. As can be seen from the comparison in Table I with conventional stellarators and torsatrons with planar axes, the heliac is naturally suited to have a stable equilibrium with high beta, due to its large rotational transform and magnetic well.

The formation of magnetic surfaces in the heliac can easily be understood using a magnetic island model. If the toroidal

TABLE I. COMPARISON OF HELIAC AND PLANAR MAGNETIC AXIS STELLARATORS AND TORSATRONS

	Heliac axis	Planar axis
Magnetic well with large transform	Yes	No
Magnetic well without toroidal shift	Possible	No
High global shear	No	Possible
High local shear	Yes	Yes
Expected beta limit	$\beta > 20\%$	$\beta \lesssim 8\%$

field coils were not placed to provide a helical component, the field would be axisymmetric with  $B_p \propto r^{-1}$  decreasing outward from the central conductor, corresponding to a rotational transform  $\chi \propto r^{-2}$ . The helical distortion of the field resonates with the magnetic field lines on and near where  $\chi_s = N$ , creating a magnetic island similar to those created in a tokamak by tearing modes. The surfaces in the central region of this island are used for plasma confinement.

This model gives a rough estimate of the rotational transform in the heliac. A magnetic field line at the resonance point goes around the central conductor  $N$  times and closes on itself after going once around the torus. Due to the  $r^{-2}$  dependence of the transform associated with the toroidal conductor, a line further out will not complete the  $N$  circuits, and one on the inside will have completed the  $N$  circuits before getting around. An estimate of this precession shows that the transform per period has the following approximate dependence on the shape of the magnetic surfaces:

$$\tau_h \approx 2w/h \quad (1)$$

where  $w$  is the width and  $h$  is the height of a surface. The rotational transform  $N$  associated with the twisting of the surface about the central coil must be added to this, so that

$$\tau = N(1 - \tau_h) \quad (2)$$

Note that these two rotations are in opposite directions. The first term in Eq. (2) is the familiar transform associated with the torsion of the magnetic axis. The second term is the one that provides a transform in stellarators with planar axes.

## 2.1. Equilibrium

The primary equilibrium issues are the quality of the magnetic surfaces and the limits on plasma beta at which the shift of the magnetic axis becomes too large. The axis shifts due to both toroidicity and helicity, but the helical shift preserves the fundamental heliac symmetry. Equilibrium properties such as magnetic well, short connection length, large local shear, and controlled magnetic ripple are needed for stability and transport considerations.

The quality of the magnetic surfaces is destroyed by magnetic perturbations resonating with the rotational transform. If  $n$  and  $m$  are toroidal and poloidal mode numbers associated with the perturbation field, magnetic islands will develop and the surfaces will be destroyed near where  $\iota = n/m$ . In the heliac, the dominant toroidal mode number is  $N$ , the number of periods. If the transform per period is small,  $\iota/N < 1/3$ , then the smallest resonant poloidal mode number is  $m = 4$ . Since the amplitudes of the magnetic perturbations are generally exponentially small for large  $m$  and  $n$ , the region of surface destruction can be limited. In the magnetic-island model of the heliac, the rotational transform is almost constant from the magnetic axis to near the separatrix that bounds the plasma region. Near the separatrix it rises to  $\iota = N$ . Attractive vacuum-field heliac configurations have been found with the rotational transform per period in the range  $0.2 \lesssim \iota/N < 0.4$  over the plasma region. Magnetic surfaces like those given in Fig. 3 obtained with a helically invariant ( $R/a \rightarrow \infty$ ) model, show that the global shear is small even at  $\beta = 20\%$  (Fig. 4). With these rotational transforms, low-order resonances can be avoided.

The equilibrium beta limit is reached when the Pfirsch-Schlüter current causes such large toroidal and helical shifts of the magnetic axis that high quality surfaces are lost. The toroidal shift, which is symmetry breaking, can be reduced with appropriate field design. To investigate the Pfirsch-Schlüter current, it is useful to adopt a Hamada-like coordinate system  $\Psi, \theta, \zeta$  in which the magnetic field lines are straight. In such a system, one can define and evaluate parameters  $\delta_{nm}$ , such that

$$\frac{1}{B^2(\Psi, \theta, \zeta)} = \frac{1}{B_0^2(\Psi)} \left\{ 1 + \sum'_{n,m} \delta_{nm} \exp[i(n\zeta - m\theta)] \right\} \quad (3)$$

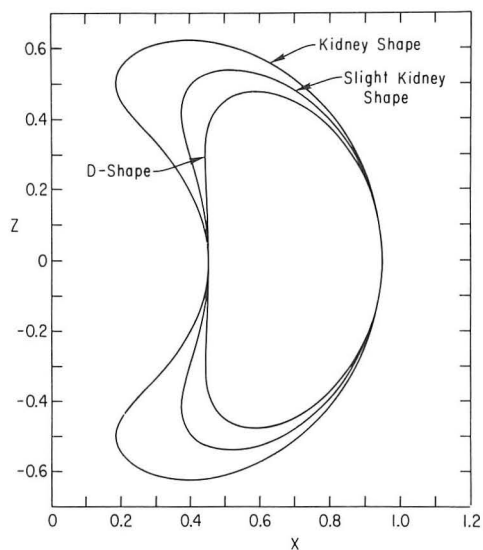


FIG.3. Magnetic surfaces in a straight heliac.

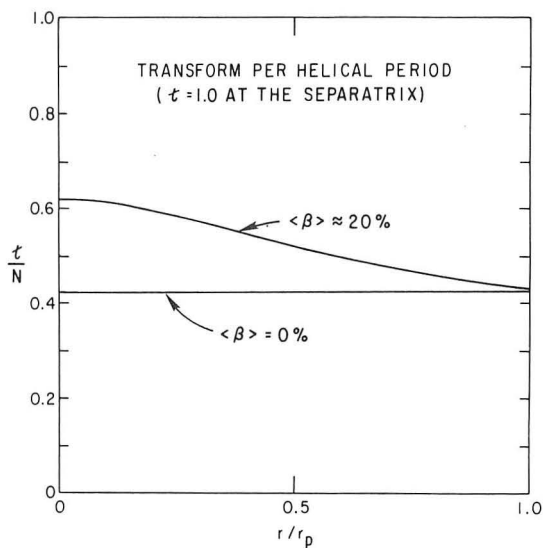


FIG.4. Rotational transform for straight heliac.

The prime implies that  $n = 0, m = 0$  is excluded. This Fourier decomposition can be evaluated numerically [13,14]. The Pfirsch-Schlüter current is

$$\frac{j_{\parallel}}{B} = \frac{cg}{2} \frac{dP}{d\Psi} \sum_{n,m} \frac{n\delta_{nm}}{n-m\kappa} \exp[i(n\zeta - m\theta)] \quad (4)$$

with  $P(\Psi)$  the pressure,  $cg(\psi)/2$  the total poloidal current outside a flux surface, and  $c$  the speed of light. This will be large near resonant surfaces where  $n = m\kappa$  unless  $\delta_{nm}$  is small, and will create a magnetic field with this resonant behavior. If we visualize an expansion technique for determining the magnetic surfaces from  $\vec{B} \cdot \nabla \Psi = 0$ , we can see that  $\Psi^{(1)}$  must be related to  $\Psi^{(0)}$  by another  $1/(n-m\kappa)$  factor. The condition that the magnetic axis is not shifted too close to the plasma surface provides a restriction,

$$\beta \lesssim 2(a/R)^2 (n-m\kappa)^2 / |\delta_{nm}| \quad (5)$$

with  $a$  the mean plasma radius and  $R$  the major radius. Note that  $\delta_{01} = 2a/R$  for an axisymmetric tokamak, so this reduces to the usually quoted equilibrium condition for  $n = 0, m = 1$ . For tokamaks, planar axis stellarators, and heliacs with a low value of  $N$ , the limitations associated with the toroidal shift ( $n=0, m=1$ ) set the  $\beta$  limit. For heliacs with  $N \gtrsim 3$ , the helical shift is usually more important. An approximate  $\beta$  limit, where the helical shift is half the plasma radius, is

$$\beta \lesssim \epsilon_h \kappa_h^2 \quad (6)$$

with  $\epsilon_h$  the ratio of the plasma half width  $w/2$  to the distance from the central coil to the magnetic axis, and the estimate  $\delta_{01} = 2(Na/R)^2 / \epsilon_h$ . In Fig. 5 the axis shift is given versus beta for the helically symmetric equilibrium of Fig. 3. Using the vacuum-field values for  $\epsilon_h$  and  $\kappa_h$ , one would analytically expect a beta limit of about 18%, which is a reasonable estimate. The validity of the simple analytic formula, Eq. (6), is illustrated by Fig. 6, constructed for a system with  $\kappa/N = 0.25$  with a three-dimensional computer code. These equilibria were not optimized to reduce the toroidal shift. A reduction could be achieved by modifying this field structure to minimize the  $\delta_{01}$  component.

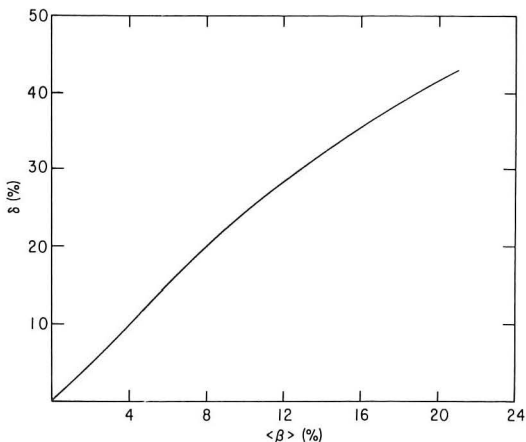


FIG. 5. Helical magnetic axis shift for straight heliac.

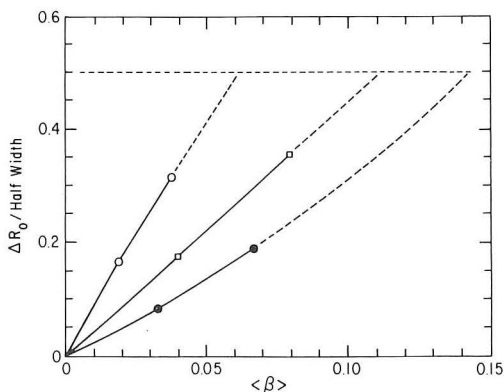


FIG. 6. Toroidal magnetic axis shift for finite-aspect-ratio heliac. The three curves from top to bottom are: for  $R/a = 4, N = 2$ ;  $R/a = 8, N = 4$ ; and  $R/a = 8, N = 6$ . No attempt was made to minimize  $\delta_{01}$  in these models.

## 2.2. Stability

The equilibrium properties of the heliac that are important for stability considerations are the magnetic well, the local and global shear, and the connection length. These quantities are quite different for configurations with large  $N$ ,  $N \gtrsim 3$ , from those with  $N \lesssim 2$  which have properties more closely resembling conventional stellarators and torsatrons. For example, the magnetic well is related to the magnetic field-line curvature.

The ratio of the helical curvature to the toroidal curvature is approximately the ratio of the field strength components  $\delta_{N1} / \delta_{01}$  of Eq. (3). This ratio scales as the number of periods, and for typical configurations is about one for  $N=3$ . For  $N=2$  then, one expects the well to be created primarily by toroidal effects, and a truly three-dimensional stability analysis is essential. The connection length between good and bad curvature regions is  $L = R/\kappa$  for toroidal curvature and  $L_h = R/N\kappa_h$  for helical curvature, with  $R$  the major radius. Since both  $R$  and  $\kappa$  are proportional to  $N$ , the connection lengths are independent of the number of periods. Their ratio,  $L/L_h = \kappa_h / (\kappa(1-\kappa_h))$ , is somewhat larger than one. The short connection lengths, together with the large local shear, stabilizes pressure-driven ballooning modes even at high beta. For high  $N$ , the equilibrium properties, including the magnetic well, are controlled by the helical fields and the stability picture should closely resemble that of a helically invariant device.

Considerable numerical work has been performed on helically symmetric models of heliac. Helical equilibria with  $\beta > 20\%$  have been found which are stable to all ideal fixed-boundary modes and resistive interchanges. The magnetic well, the strong local shear, and the short connection length are all stabilizing features of the heliac geometry. Although the global shear,  $dx/d\psi$ , is small, the shear in the field lines is strong on both the concave and convex sides of the kidney-shaped magnetic surfaces. In other words, the local shear is large but its average is almost zero.

### 2.3. Transport

Heliacs, like other asymmetric configurations, can have large diffusion coefficients both for the electrons and the ions. However, nonclassical scattering could greatly reduce the effects of asymmetry on the electron transport and actually improve confinement.

The heliac has some attractive transport features. In the large-aspect-ratio limit, the helical variation  $\delta_{N1}$  of the field strength dominates over the other components, including toroidal effects. Since high-beta stability is maintained in the large  $R/a$  limit of the heliac, there may be a further benefit from the symmetrizing effect of the plasma self-well. In this limit, neoclassical transport should be as good as, or better than, that calculated for axisymmetric systems [15]. In other stellarator designs, where the magnetic well depends on toroidicity, the

helical and toroidal ripples must be comparable. It is clear that high-grade confinement could be achieved with large-aspect-ratio heliacs,  $R/a \approx 100$ . Preliminary Monte-Carlo studies using exact vacuum magnetic fields indicate that adequate ion confinement for a reactor should be achievable in heliacs with  $R/a \approx 20$ .

### 3. CONCLUSION

The superposition of helical fields on a tokamak can provide an additional vacuum rotational transform that enhances stability by strengthening the poloidal field in the region of unfavorable curvature. The tokatron is particularly well suited for this role because of its symmetry-conserving geometry and simple modular coil structure.

In a heliac, the poloidal field from a current-carrying toroidal ring combines with an  $\ell = 1$  helical field. This provides a strong magnetic well even in the absence of toroidicity. The current-carrying toroidal conductor provides a shorter connection length between regions of unfavorable and favorable curvature and larger local shear than that in a conventional stellarator or torsatron. Thus, a heliac has a smaller shift of the magnetic axis, a higher equilibrium beta, and better stability and transport properties than those of stellarators and torsatrons.

#### Acknowledgment

This work was supported by United States Department of Energy Contract No. DE-AC02-76-CH03073.

#### REFERENCES

- [1] FURTH, H.P., HARTMAN, C., Phys. Fluids 11 (1968) 408.
- [2] IKEZI, H., SCHWARZENEGGER, K.F., LUDESCHER, C., Phys. Fluids 22 (1979) 2009.
- [3] ANANIA, G., private communication (to be published).
- [4] SHEFFIELD, G.V., FURTH, H.P., Princeton Univ. Plasma Physics Lab. Rep. PPPL-1827 (1981) unpublished.
- [5] FURTH, H.P., KILLEEN, J., ROSENBLUTH, M.N., COPPI, B., in Plasma Physics and Controlled Nuclear Fusion Research 1965 (Proc. 2nd Int. Conf. Culham, 1965) Vol. 1, IAEA, Vienna (1966) 103.
- [6] SOLOV'EV, L.S., SHAFRANOV, V.D., Rev. Plasma Phys. 5 (1970) 188.
- [7] YOSHIKAWA, S., Princeton Univ. Plasma Physics Lab. Annual Report 1981; Institute of Plasma Physics, Nagoya University, Rep. US-J FRC-005 (1981) unpublished.
- [8] SPITZER, L., Jr., Phys. Fluids 1 (1958) 253.

- [9] FÜNFER, E., KAUFMANN, M., LOTZ, W., NEUHAUSER, J., in Plasma Physics and Controlled Nuclear Fusion Research 1971 (Proc. 4th Int. Conf. Madison, 1971) Vol. 3, IAEA, Vienna (1972) 189.
- [10] NAGAO, S., WATANABE, H., KOYAMA, K., in Proc. 3rd. Topical Conf. High-Beta Plasmas, Pergamon Press (1976) 369.
- [11] DREMIN, M.M., SOLNTSEV, A.M., STEFANOVSKIJ, A.M., in Plasma Physics and Controlled Nuclear Fusion Research 1976 (Proc. 6th Int. Conf. Berchtesgaden, 1976) Vol. 2, IAEA, Vienna (1977) 169.
- [12] GRUBER, R., KERNER, W., MERKEL, P., NÜHRENBERG, J., SCHNEIDER, W., TROYON, F., Comput. Phys. Commun. 24 (1981) 389.
- [13] BOOZER, A.H., Phys. Fluids 25 (1982) 520.
- [14] KUO-PETRAVIC, G., BOOZER, A.H., ROME, J.A., to be published.
- [15] PYTTE, A., BOOZER, A.H., Phys. Fluids 24 (1981) 88.

## DISCUSSION

H. WOBIG: How large is the variation of the field strength on the magnetic axis?

S. YOSHIKAWA: The case in Fig.1 could have field variations as low as 2% or less. Other configurations also could have low field variation (less than 10%) on the magnetic axis.

H. WOBIG: What trapped-particle losses do you expect, and how do they compare with conventional stellarators and torsatrons?

S. YOSHIKAWA: We have not exhaustively analysed this yet.

A.H. BOOZER: I should like to add that the ripple on the magnetic axis can be made arbitrarily small. In this case the ripple increases approximately linearly with distance from the axis and so the question of trapped-particle confinement is important. Preliminary results indicate that adequate reactor confinement should be obtained at a reasonable aspect ratio.

F.L. RIBE: Dr. Yoshikawa, do you prefer the figure-8,  $N = 2$  system or a higher  $N$  number for the heliac?

S. YOSHIKAWA: I think high  $N$  is preferable.

F.L. RIBE: Could you please comment on the stability  $\langle\beta\rangle$  limit for large ( $\rightarrow\infty$ ) aspect ratio?

S. YOSHIKAWA: The stability limit is calculated to be at 20% or beyond. The equilibrium  $\beta$  is almost 100%.

F.L. RIBE: Do you obtain equally favourable  $\langle\beta\rangle$  limits for the planar (snake) axis as for the non-planar (helical) axis?

S. YOSHIKAWA: I presume so, but we have not analysed this.

# PLASMA PHYSICS AND CONTROLLED NUCLEAR FUSION RESEARCH 1982

NINTH CONFERENCE ON PLASMA PHYSICS  
BALTIMORE, MARYLAND, SEPTEMBER 1982

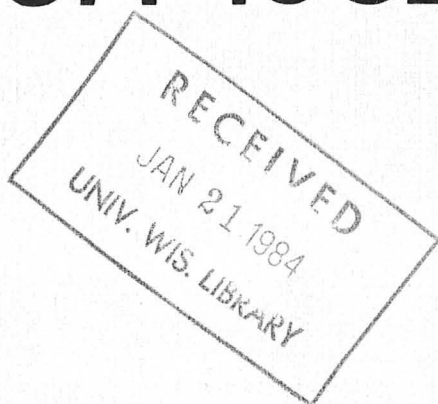
## VOL. III

NUCLEAR FUSION RESEARCH REPORT

LEWIS F. WENDT LIBRARY  
COLLEGE OF ENGINEERING

FEB 24 1984

UNIV. MADISON, WI 53706



INTERNATIONAL ATOMIC ENERGY AGENCY, VIENNA, 1983